Excitation of the 4*d* shell in Sb, Te, and BaF_2 with inelastic electron scattering: Collective or single particle?*

Carl Franck and S. E. Schnatterly
Department of Physics, University of Virginia, Charlottesville, Virginia 22901
(Received 8 December 1981)

Simple models suggest that the momentum-transfer (q) dependence of inelastic electron scattering is sensitive to the difference between collective and single-particle behavior in atomic dynamics. We measured the energy centroid of the 4*d* continuum peak for $0 < q \leq 1.4$ Å^{-1} in the following solids having complete 4*d* shells: Sb, Te, and BaF_2, and find that a single-particle description is favored.

I. INTRODUCTION

The complete 4*d* shell has become an arena for theories of electron correlation in atoms. Models have been tested by comparison with continuum photoabsorption measurements on Xe and its neighbors in the periodic chart.[1] The failure of certain single-particle models to describe these spectra is well documented. While one such model, based on the Hartree-Fock-Slater potential, shows some shift in the peak of continuum oscillator strength away from threshold, it does not go far enough to agree with experiment.[2] Furthermore, the continuum bump in Xe is much broader than this single-particle model predicts.

By including statistical correlations inside the 4*d* shell, a Hartree-Fock (HF) calculation by Kennedy and Manson approaches the measured continuum in Xe.[3] Recent HF theories by Kelly, Carter, and Norum have given fair agreement with Ba 4*d* measurements while emphasizing the importance of relaxation effects.[4] In Xe, Amusia uses an infinite-order perturbation scheme called random-phase approximation with exchange (RPAE) to find good agreement with experiment.[5] The best descriptions of 4*d* photoionization in Ba are provided by Kelly's use of ground-state correlation in finite-order perturbation theory,[6] Wendin's RPAE with relaxation,[7] and the recent time-dependent density-functional approach of Soven and Zangwill.[8] An intriguing interpretation of the 4*d* continuum peak in Xe is provided by Amusia and Wendin.[5,7] For them, it signals the occurrence of collective oscillatory notion in the 4*d* shell—an atomic analog of giant dipole resonances in nuclei and plasmons in metals.

II. INELASTIC ELECTRON SCATTERING

The above approaches are based on rather divergent points of view, yet all but the simplest can produce reasonable agreement with the measured spectra. Here we describe results of an additional experiment, inelastic electron scattering, which can provide a new parameter to be used in distinguishing between the above theoretical approaches.

Our experimental objective is the measurement of "dispersion" in the 4*d* continuum. Our operational definition of dispersion is the shift in the energy centroid of the 4*d* continuum $\langle E \rangle_{4d}$ as a function of momentum transfer q.

In our scattering experiment, we measure the rate of transfer of momentum $\vec{q}$, and energy $E(=\hbar\omega)$, from a fast electron beam to a thin-film target. Our work is similar to earlier experiments that studied 4*d* excitations in gaseous XE over a q range of from 0.5 to 5.4 Å^{-1}.[9] In a given experimental run we fix the scattering angle θ, while the scattered beam is counted as a function of E, the energy loss in the target.

For E and q which are small compared to the incident energy and momentum, q is given by

$$q^2 \approx \left[\frac{m^2E^2}{\hbar^2k_o^2}\right] + \left[k_o^2\theta^2\right], \tag{1}$$

where k_o is the outgoing projectile momentum. Since the first term can be made small compared to the second term at sufficiently large scattering angles, q and E can be decoupled.

The differential scattering cross section can be expressed three ways. First, Fermi's golden rule gives[10]

$$\frac{d\sigma}{dE\,d\Omega} \propto \frac{|\langle f|e^{i\vec{q}\cdot\vec{r}}|i\rangle|^2}{q^4};$$

$d\Omega$ is the differential scattering angle. The born approximation is valid since the incident beam energy, 300 keV, is large compared to the characteristic energies to be examined. A power-series expansion in q of the transition operator, $e^{i\vec{q}\cdot\vec{r}}$ reveals that as q is increased from zero, monopole and quadrupole as well as dipole excitations are created in a localized system.

At this point, we can derive a result which will guide us later. We show that the energy centroid $\langle E\rangle$ of an atom's entire spectrum is an even function of q. We use a second expression for the differential cross section[10]

$$\frac{d\sigma}{dE\,d\Omega} = \frac{4\hbar}{a_0^2 q^4} S(q,\omega) .$$

$S(q,\omega)$ is the dynamic structure factor. We are interested in the quantity

$$\langle E\rangle \equiv \frac{\int_0^\infty \frac{d^2\sigma}{d\Omega\,d\omega}\hbar\omega\,d\omega}{\int_0^\infty \frac{d^2\sigma}{d\Omega\,d\omega}d\omega}$$

$$= \frac{\int_0^\infty S(q,\omega)\hbar\omega\,d\omega}{\int_0^\infty S(q,\omega)d\omega} .$$

The numerator is given[10] by the f-sum rule

$$\int_0^\infty \omega S(q,\omega)d\omega = Zq^2/2m .$$

The denominator, which is called the instantaneous structure factor, is given by[10]

$$S(q) = \frac{1}{\hbar}\left\langle 0\left|\sum_{ij} e^{-i\vec{q}\cdot\vec{r}_i} e^{+i\vec{q}\cdot\vec{r}_j}\right|0\right\rangle .$$

The sum is over all the electrons in the atom, their positions being r_i, r_j. Now, we have

$$\langle E\rangle = \frac{Zq^2}{2mS(q)} . \tag{2}$$

To show that $\langle E\rangle$ is an even function of q, all that is necessary is to show that $S(q)$ is even. But this is obvious, since replacing $\vec{q}$ with $-\vec{q}$ and switching labels i and j in the expression for $S(q)$ returns the same result.

A third interpretation of the differential cross section is in terms of the energy and wave-vector-dependent dielectric function for longitudinal response $\hat{\epsilon}_L$ (Ref. 10):

$$\frac{d\sigma}{dE\,d\Omega} \propto \frac{1}{q^2}\mathrm{Im}\left[-\frac{1}{\hat{\epsilon}_L(q,E)}\right] . \tag{3}$$

We will use this expression in order to normalize our measurements.

III. EXPERIMENT

A description of our inelastic electron scattering spectrometer has been published.[11] At our incident beam energy of 300 keV, the attenuation length is on the order of 1000 Å in solid Te. Consequently, we prepared thin evaporated films as targets. The Te and Sb specimens were prepared as thin as 200 Å, and were supported on a copper wire screen. Our thinnest BaF_2 sample, 480 Å thick, was on a carbon film substrate again held by a copper screen. We cover an energy-loss range of $0 < E \leq 300$ eV with a fixed resolution in the range $0.1 \leq \Delta E \leq 0.3$ eV. The useful q range, limited by quasielastic-inelastic multiple scattering, is $0 < q \leq 1.4$ Å^{-1}. Since the size of a $4d$ orbital is $\langle r\rangle_{4d} \approx 0.5$ Å, we have sufficient momentum transfer to vary the selection rules for transitions from this shell.

Our experimental program is as follows. We measure the scattering rates in the range of the $4d$ excitation for each of the three materials at various scattering angles. We then apply a small correction to the spectra to account for the E dependence of q seen in Eq. (1). This allows us to regard q as the momentum transfer that is perpendicular to the primary beam direction only. Next we extract the centroid of the $4d$ continuum bump $\langle E\rangle_{4d}$. The difficult step in this procedure is to remove the background contribution to the rate caused by excitations of electrons with binding energy less than that of the $4d$ electrons. We therefore begin by performing a background fit. We then extract the $4d$ centroid by background subtraction and moments analysis of the difference. This procedure was carried out in several different ways to allow an estimate of the uncertainties involved. Finally, given $\langle E\rangle_{4d}$, we look for its change with q.

Examples of $4d$ spectra with fitted backgrounds[12] for the three materials studied are shown in Fig. 1. In Sb and Te the continuum bump appears as a broad peak centered about 40 eV above the sharp lines at threshold. The small modulations at the peak could be solid-state effects, as seen in the gas- and solid-photoabsorption studies of Xe.[1(b)] In BaF_2 the continuum bump is more asymmetric, with more severe modulations. From

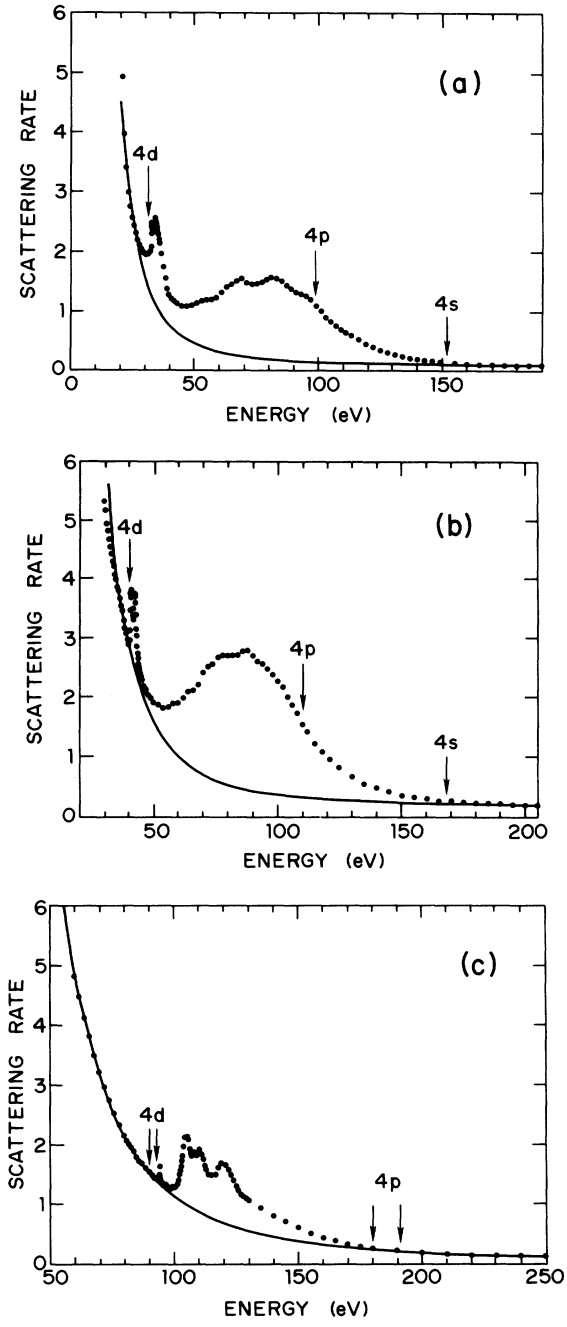

FIG. 1. Inelastic electron scattering spectra of the 4d shell; rate (arbitrary units) vs energy (E). Solid lines are background fits. Atomic binding energies are indicated. (a) Sb, 200 Å thick, $q=0.8$ Å^{-1}; (b) Te, 200 Å thick, $q=1.0$ Å^{-1}; (c) BaF_2, 480 Å thick, $q=1.1$ Å^{-1}.

comparison with vapor phase Ba photoaborption results,[1(c)] we conclude that these wiggles are not atomic in origin. In all materials, the background due to excitations with low-energy thresholds contributes a significant cross section which falls with increasing energy across the 4d region. We do not detect additional features near the 4p and 4s binding energies (as given by Ref. 13).

By applying a Kramers-Kroning transformation to our $q=0.3$-Å^{-1}, 200-Å-thick Te spectrum, we can generate absolute values for the real and imaginary part of the dielectric function [see Eq. (3)].[14] We normalize the spectrum with the aid of a low-frequency measurement: At $E=0.3$ eV, $\mathrm{Re}(1/\hat{\epsilon})\approx 0.03$ which we take to be zero.[15] Our value of the photoabsorption coefficient over the 4d region is in good agreement with synchrotron measurements.[16] In making this comparison, we have relied on the fact that at low momentum transfers, the transverse dielectric function measured in photoabsorption and the longitudinal dielectric function provided by inelastic electron scattering are the same.[17]

To see how important multiple scattering is to our observations, we calculate the effective number of electrons per atom, n^*, for different target thicknesses[18]:

$$\int_{4d} E\epsilon_2(E)dE=\frac{2\pi^2\hbar^2 N_a e^2}{m}n^* , \tag{4}$$

where N_a is the number density of atoms,[19] e the electron charge, and m the electron mass. The integral is over the 4d portion of the spectrum ($39\leq E\leq 250$ eV for Te). We get $n^*=12.3$ electrons per atom for a 200-Å-thick target and $n^*=16.3$ electrons per atom for a 400-Å-thick Te target (both for $q=0.3$ Å^{-1}). We see that multiple scattering can be important. We will discuss the effects of multiple scattering on our dispersion measurements below.

IV. DISPERSION ANALYSIS

Returning to the question of how the centroid of the 4d continuum changes with momentum transfer, we discuss our first method of centroid extraction—background fit followed by moments analysis.

We take the regions, given in Table I, for our background fits to the function

$$R_b=\alpha_1 E^{-\alpha_2}+\alpha_3 . \tag{5}$$

We divide the measured spectrum into three regions: one below the 4d threshold which is due to the background alone, a central region containing

TABLE I. Intergration regions for background fits and moments analysis.

Material	4d threshold (eV)	Background-fit regions (in eV)	Moments integration region (in eV)
Sb	33	(22.4, 25.4)(170, 190)	[49.0, 165]
Te	41	(37.5, 39.5)(185, 205)	[39.5, 180]
BaF_2	91	(83.0, 92.2)(210, 250)	[90.0, 230]

the 4*d* continuum resonance, and a region well above the resoncance which we take to be dominated by the background. These three regions are listed in Table I. The crucial choice is the lower limit E_0 to the threshold region. We computed the 4*d* centroid ($\langle E \rangle_{4d}$) for various values of E_0. We use E_0 values for which $\langle E \rangle_{4d}$ is not significantly changed by small changes in E_0. In the case of Sb, we are careful to stay below the energy region in which double scattering of the 15-eV solid-state plasmon loss might occur.

We find values of α_2 in Eq. (5) that are in the range 2–3 for low-q values. This appears reasonable since one generally expects $\alpha_2 \approx 3$ for the high-energy tail of an electron scattering spectrum. Assuming only counting uncertainties in the spectra, the χ^2/ν (chi squared divided by number of degrees of freedom) values for the fits over the $0 < q \leq 1.4$-Å^{-1} range are as follows: for Sb, $2 < \chi^2/\nu < 48$ for Te, $0.2 < \chi^2/\nu < 11$, and the BaF_2, $2 < \chi^2/\nu < 13$. In view of the poor fits, we inflate the estimated data point uncertainties in order to give $\chi^2/\nu = 1$.

With a background function in hand, we are able to strip away the spectrum due to low threshold excitation and leave an approximate 4*d* spectrum (R_{4d}). That is,

$$R_{4d} = R_{\text{meas}} - R_b \ .$$

Next, we evaluate the centroid of R_{4d}:

$$\langle E \rangle_{4d} = \frac{\int E R_{4d} dE}{\int R_{4d} dE} \ .$$

The moments integration regions used are given in Table I. In Sb, we start well past 30 eV in order to avoid the strong double-scattering region. In computing the uncertainty in $\langle E \rangle_{4d}$, we include the correlated error in each data point arising from the use of a background function.[20] The background-fit contribution to the error in $\langle E \rangle_{4d}$ greatly exceeds that due to electron counting uncertainty in the measurements.

Using Eq. (4), we calculate the effective number of electrons in the 4*d* bump. For a Te, 200-Å-thick target, $q = 0.3$ Å^{-1}, with background removed we find $n^*_{4d} = 9.5$ electrons per atom. From our measurements of integrated oscillator strength for different thicknesses, we estimate an uncertainty of 3 electrons per atom to this value. Since most of the 4*d* shell's ten electrons worth of oscillator strength is found in the continuum bump, we conclude that this shell does not interact strongly with the rest of the atomic electrons. Our measurement is therefore consistent with the continuum bump being a feature of *intra*shell interaction.

Taking up our results for $\langle E \rangle_{4d}$ versus q, we use the following form for our low-q data:

$$\langle E \rangle_{4d} = c + (dq^2) \ , \tag{6}$$

where c and d are constants, d being the interesting coefficient of dispersion. We are guided to this expression for low-q dispersion by our proof that, in averaging over the entire spectrum, $\langle E \rangle$ is an even function of q. Therefore, we drop the linear term in q from a power-series expansion. Equation (6) is also the form predicted by all the models we have studied. Table II (moments analysis) gives our fits to Eq. (6) using the above analysis. We use $0 < q \leq 1.4$ Å^{-1} in order to avoid confusion due to inelastic-quasielastic multiple scattering. Since the χ^2/ν values are large, we again inflate the errors to produce unity for χ^2/ν. This gives the errors σ'_d for the dispersion coefficient. In both Te and Sb we find agreement for 200- and 400-Å-thick samples. Therefore multiple scattering does not appear to present a problem for our dispersion measurements at low q (≤ 1.4 Å^{-1}). The dispersion is largest for Te and about the same for Sb and BaF_2.

In Figs. 2–4, we show the dispersion extracted by the moments analysis in Sb, Te, and BaF_2, respectively. The uncertainties in the centroids correspond to a $\chi^2/\nu = 1$ for the background fits. Note the effect of inelastic-quasielastic multiple scattering for $q^2 \geq 2$ Å^{-2}. The best-fit line corresponds to Eq. (6).

TABLE II. Dispersion results (see text for explanation).

Material	Thickness (Å)	Moments analysis χ^2/ν	d(eV/Å^{-2})	σ_d	σ_d'	Gaussian fit χ^2/ν	d(eV/Å^{-2})	σ_d	σ_d'	d_1	d_2
Sb	200	60/7	1.24	0.12	0.35	16/7	−2.4	0.3	0.5	(−4,−2)	(−3.2,−1.6)
Sb	400	16/8	0.96	0.13	0.18	6.3/8	−2.0	0.3	0.3		
Te	200	26/9	3.66	0.33	0.56	39/9	2.1	0.2	0.4	(1.6,2.8)	(1.2,3.0)
Te	400	19/6	5.37	0.60	1.07	24/6	3.4	0.4	0.8		
BaF_2	480	15/3	1.50	0.20	0.45						

As a check on our moments-analysis results, we recompute $\langle E \rangle_{4d}$ versus q^2 using a Gaussian plus background fit. This is an inferior method since it presupposes a particular shape for the continuum. We find that for Sb and Te, both Gaussian and Lorentzian shapes give usable fits. However, the complicated asymmetric shape of the 4d continuum in BaF_2 puts it beyond the reach of this method.

Our Gaussian-fit procedure is as follows: First, we fit the background in the same manner as was used in the moments analysis, Then we fit the continuum line shape over the integration regions given in Table I with

$$R = R_b + \alpha_3 \exp[-\alpha_4 (E - \alpha_5)^2] .$$

By keeping the background fixed, we ignore the nonphysical contribution to the Gaussian shape by points below the 4d energy threshold.

The advantage of the Gaussian-fit method is that it helps us to understand the contribution of potential systematic errors. We can look for changes in the dispersion coefficient caused by varying the range of the fit. The two crucial parameters are the lower limit of the high-energy fit region, and the centroid of the low-energy background region. The range of variation of the dispersion coefficient for small, reasonable variations of these parameters are given by d_1 and d_2, respectively, in Table II (Gaussian fit). The results are consistent.

Our Gaussian-fit dispersion results are given under d in Table II. The errors σ_d are derived from the fits to Eq. (6). Taking $\chi^2/\nu = 1$ for these

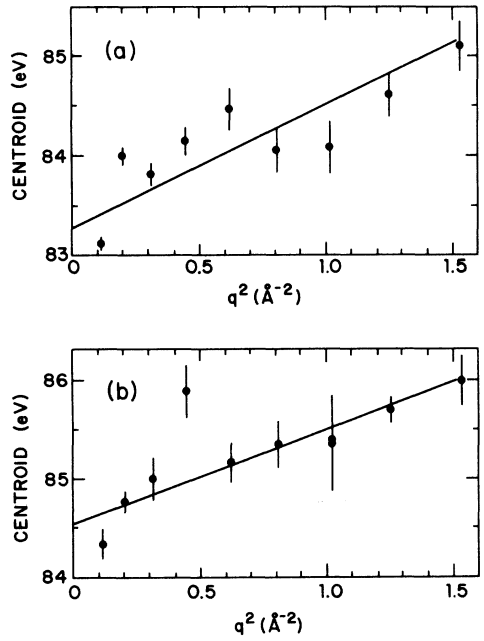

FIG. 2. Energy centroids vs q^2 for Sb using moments analysis: (a) 200-Å thick target; (b) 400-Å thick target.

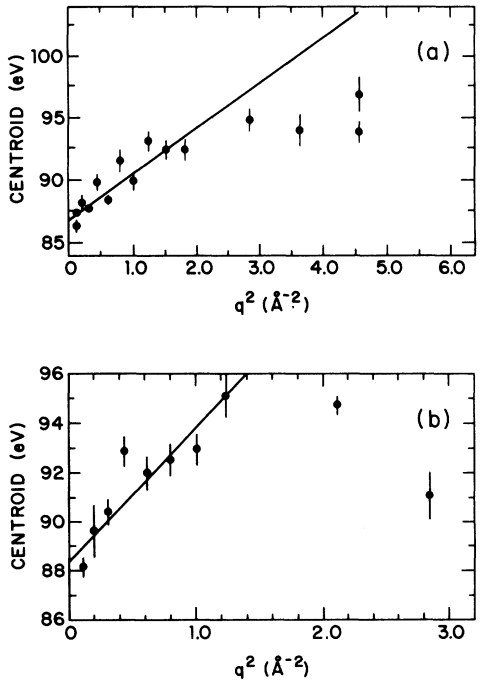

FIG. 3. Energy centroids vs q^2 for Te using moments analysis: (a) 200-Å thick target; (b) 400-Å thick target.

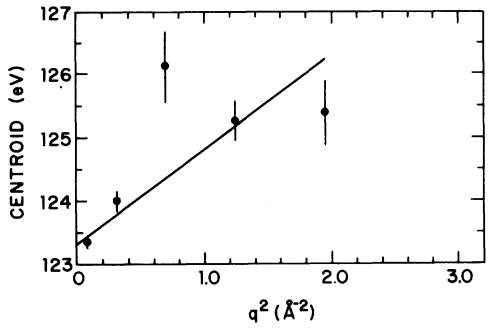

FIG. 4. Energy centroids vs q^2 for BaF_2 using moments analysis. 480-Å thick target.

fits gives the final errors σ_d'.

In conclusion, the Gaussian-fit method gives us a sense of the variation of the measured dispersion with fitting method. As in the case of the moments analysis, it gives agreement for different target thicknesses. The dispersion coefficient values agree with the moments analysis for Te, but not for Sb. Possibly the increased double-plasmon contribution at low energies in Sb accounts for this variance.

In conclusion, we rely on the moments analysis to supply the measured dispersion. We find agreement for different thicknesses in Te and Sb indicating that multiple scattering is not a problem. A second method of reducing the data, a Gaussian fit, suggests that uncertainties in the dispersion coefficient may be as large as ± 1 eV Å^2. The dispersion in Sb and BaF_2 is small, ≈ 1 eV Å^2. For Te it is ≈ 4 eV Å^2.

V. MODELS

In order to appreciate the significance of our dispersion measurements in understanding 4*d* correlations, it is necessary to find out what various single-particle and collective models predict. We derive inelastic electron scattering results for Te in one very simple model of each type. While neither is capable of explaining photoabsorption measurements, they suggest the degree to which our experiments are sensitive to correlations in 4*d* electronic motion. More sophisticated approaches to the calculation of atomic dispersion are feasible. An important example is Amusia's RPAE prediction of inelastic electron scattering in Xe.[21]

For our single-particle model, we assume a Hartree-type atom composed of a complete 4*d* shell of hydrogenic orbitals around a core with $+10e$ charge, and compute the dispersion using Eq. (2). Use of a product wave function for the ground state allows us to express $S(q)$ in terms of the expectation values of the single-particle orbitals of the fully occupied 4*d* shell[10]:

$$S(q)=Z-\sum_i |\langle i | e^{i\vec{q}\cdot\vec{r}} | i \rangle|^2 .$$

The sum is over the states of the 4*d* shell. Evaluating $S(q)$ with hydrogenic 4*d* wave functions for $Z=10$, we find the values $c=8$ eV; and $d=2.0$ eV Å^2 for small q, and $d=2.7$ eV Å^2 for the largest momentum transfer used in the experiment ($q=1.4$ Å^{-1}).

By way of comparison, we also find the 4*d* dispersion using a collective model of the excitation. In the simplest model of this type, one replaces the 4*d* shell by a metallic ball of uniform charge density. Before studying the consequences, we first check to see whether the usual criterion for plasmalike behavior is met in the 4*d* electronic system. If the ratio of average kinetic energy K, to average interparticle potential energy W is greater than or equal to one, the system is said to be a good plasma and collective charge oscillations may occur.[22] In order to evaluate the situation in Te, we calculate[23] $\langle K \rangle_{4d} = \frac{1}{2}\langle \vec{r}\cdot\vec{\Delta}V \rangle_{4d}$ using the 4*d* wave function from the Hartree-Fock-Slater model, and the atomic potential V, seen by an electron in this model.[24] We find $\langle K \rangle_{4d}=454$ eV, close to the value given by $E_{4d}=\langle K \rangle_{4d}+\langle V \rangle_{4d}$, where E_{4d} is the Hartree-Fock-Slater binding energy.[24]

To compute W we use the Hartree-Fock-Slater potential but only consider the contribution due to nine 4*d* electrons. We get $\langle W \rangle_{4d}=208$ eV. Therefore $K/W \approx 2$, a favorable ratio for plasmalike behavior.[22] Other theoretical searches for atomic plasmons have also reached positive conclusions for particular atomic systems.[25]

In our collective model for 4*d* excitations, we imagine a metal ball with a radius equal to $\langle r \rangle_{4d}=0.49$ Å (obtained using the Hartree-Fock-Slater model[24]). If the ball is filled with the ten 4*d* electrons, we have a number density of $n=20$ Å^{-3}. An alternative picture represents the 4*d* system by a metallic "shell" with mean radius $\langle r \rangle_{4d}$ and thickness:

$$\Delta r_{4d}=(\langle r^2 \rangle_{4d}-\langle r \rangle_{4d}^2)^{1/2}=0.20 \text{ Å} .$$

This gives $n=16$ Å^{-3} inside the shell. We therefore take the electron density to be in the range $16 \leq n \leq 20$ Å^{-3}.

Given this electron density, and taking the col-

lective mode energy from experiment on Te, $\langle E\rangle_{4d}=85$ eV, we compute the cutoff wave vector for Landau damping,[18] $q_L=\langle E\rangle_{4d}/v_F=1.4$ Å^{-1}, where v_F is the Fermi velocity for the derived density. The atomic 4d system is unusual as a metallic gas supporting plasma oscillations since q_L^{-1} is on the order of the size of the system (0.5 Å). This suggests that the localized collective mode mixes well with single-particle excitations. Thus we expect the collective resonance to be strongly damped. This is consistent with the large observed width.

In considering the excitations that can occur on the metal ball, we note that the primary difference between an actual metal ball and the Te 4d shell is that the Te shell has an energy gap, the 4d binding energy, E_g[=42 eV (Ref. 13)]. Therefore, we expect the energy of a longitudinal mode of excitation E_l, seen as a scattering resonance in our experiment to be different from the corresponding plasma mode energy of the metal ball E_p. We relate the two using an expression developed to connect exciton and plasmon modes in wide-gap insulators[26]:

$$E_l^2=E_p^2+E_g^2 .$$

We use the classical bulk and surface waves that can occur on a sphere as our plasma modes. Their energies are the solutions to[27]

$$\epsilon_l=-\left[\frac{l+1}{l}\right]$$

for surface waves of angular momentum l, and

$$\epsilon=0$$

for a bulk wave. For ϵ, we use the real part of the Lindhard dielectric function[28] whose parameters are supplied by a free-electron model with the density derived above.[29]

In order to compute the electron scattering spectrum, we must know the probability of excitation of these modes as a function of momentum transfer. For this we turn to work performed on x-ray and electron scattering from metal balls and voids in metals.[30,31] For low q, we have the rate for exciting l-wave surface plasmons:

$$\frac{d\sigma_l}{d\Omega}=2\pi a_0 r_0\frac{\omega_l}{R}(2l+1)^2\frac{j_l^2(qr_0)}{(qa_0)^4} ,$$

where a_0 is the Bohr radius, r_0 is the radius of the ball, R is the Rydberg constant, ω_l is the eigenenergy of the plasmon mode, j_l is a spherical Bessel function. For volume plasma waves, the low-q cross section is[30]

$$\frac{d\sigma_{vp}}{d\Omega}=\frac{r_0^3\omega_{vp}}{3a_0R}\frac{1}{(qa_0)^2} ,$$

where ω_{vp} is the volume plasmon energy.

At low momentum transfers, e.g., $q=0.2$ Å^{-1}, the $l=1$ surface wave is the dominant mode, followed by the bulk mode. At higher momentum transfers, e.g., $q=1.0$ Å^{-1}, the $l=2$ surface mode has risen in excitation probability to become second only to the $l=1$ mode. We perform a weighted average at each q to find the centroid $\langle E\rangle_{4d}$ of the spectra. One might expect that since the various modes occur at different energies, the change in relative excitation probability would account for any shifts in $\langle E\rangle_{4d}$ with q. Instead, the dominant "dispersing" mechanism is the change in the eigenenergies themselves with q. Therefore, the dispersion we predict is closely related to the q dependence of the Lindhard dielectric function. Our dispersion result in this model has the form of Eq. (6) with

$$10.9\le d\le 11.5 \text{ eV Å}^2 ,$$

$$100\le c\le 109 \text{ eV} .$$

The uncertainties reflect the range of densities described earlier.

VI. CONCLUSIONS

In Fig. 5, our measured and predicted values for d, the dispersion coefficient, are given as a function of atomic number Z. Multiple scattering does not appear to be a problem in Te and Sb since the

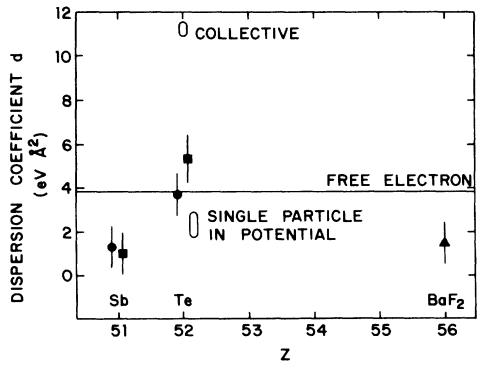

FIG. 5. Dispersion coefficient (d) vs atomic number (Z): Squares, 200-Å thick targets; circles, 400-Å thick targets; triangle, 480-Å thick target. Three models are presented.

results are independent of sample thickness.

Besides our collective- and single-particle predictions, we have included the free-electron response expected to occur at large momentum transfer. This is the regime of Compton scattering for which $qr >> 1$, where r is the radius of the $4d$ shell. This means $q^2 >> 4$ Å^{-2} while our experiments extended only up to $q^2 = 2$ Å^{-2}. The dispersion in this model is simply given by the recoil energy $\langle E \rangle = \hbar^2 q^2/2m^2$, where m is the electron mass.[32] The free-electron result $d = 3.8$ eV Å^2 is independent of Z. We find that our Te results are remarkably close to this high-q limit. Overall our measured dispersion appears to favor single-particle as opposed to collective descriptions.

To summarize, we have been able to examine $4d$ excitations with nonzero momentum-transfer inelastic electron scattering experiments in solid Sb, Te, and BaF_2 A Kramers-Kroning analysis shows that our Te spectrum is consistent with absolute photoabsorption measurements. The oscillator strength contained in the broad bump in the $4d$ continuum of this material is approximately equal to the total value expected from the $4d$ shell. We have drawn attention to the shift in the continuum centroid as a function of momentum transfer. From simple model calculations, we expect these dispersion measurements to be sensitive to whether or not collective behavior is occurring in these $4d$ excitations. Our measurements favor a single-particle interpretation.

It would be valuable to compare these dispersion results with predictions made by more realistic models which are in agreement with photoabsorption spectra. The models mentioned above, such as Hartree-Fock,[3,4] Hartree-Fock improved using many-body perturbation theory,[6] RPAE (Refs. 5 and 7), and the time-dependent density-functional approach[8] are all able to describe the ($q \approx 0$) photoabsorption spectra reasonably well. At present there is no physical basis for distinguishing between these rather different approaches to understanding $4d$-shell core spectra. The dispersion measurements presented here provide a new parameter with which these models must be consistent and which may be useful in sorting out the different effects described in these models.

ACKNOWLEDGMENTS

We especially wish to thank Patrick Gibbons for his assistance in this work. The following persons were also extremely helpful: Susan Slusky, Edward Groth, Hugh Kelly, Steve Girvin, Fred Zutavern, Tom Aton, and John Fields. This work was supported by a grant from the National Science Foundation.

---

*The experiments and much of the data analysis described here were performed while the authors belonged to the Physics Department of Princeton University, Princeton, New Jersey.

[1](a) F. J. Comes, U. Nielson, and W. H. E. Schwarz, J. Chem. Phys. 58, 2230 (1973); (b) R. Haensel, G. Keitel, P. Schreiber, and C. Kunz, Phys. Rev. 188, 1375 (1969); (c) P. Rabe, K. Radler, and H.-W. Wolff, in *Vacuum Ultraviolet Radiation Physics,* edited by E. E. Koch, R. Haensel, and C. Kunz (Pergamon Braunschweig, West Germany, 1974), p. 247.

[2]J. W. Cooper, Phys. Rev. Lett. 13, 762 (1964).

[3]D. J. Kennedy and S. T. Manson, Phys. Rev. A 5, 227 (1972).

[4]Hugh P. Kelly, Steven L. Carter, and Blaine E. Normum, Phys. Rev. A 25, 2052 (1982).

[5]M. Ya Amus'ya, N. A. Cherepkov, and L. V. Chernysheva, Zh. Eksp. Teor. Fiz. 60, 160 (1971) [Sov. Phys.—JETP 33, 90 (1971)]; M. Ya Amusiya, in *Vacuum Ultraviolet Radiation Physics,* edited by E. E. Koch, R. Haensel, and C. Kunz (Pergamon, Braunschweig, West Germany, 1974), p. 205.

[6]H. P. Kelly, in *Photoionization and Other Probes of Many-Electron Interactions,* edited by F. J. Wuilleumier (Plenum, New York, 1976), p. 83.

[7]G. Wendin, J. Phys. B 6, 42 (1973); G. Wendin, in *Photoionization and Other Probes of Many-Electron Interactions,* edited by F. J. Wuilleumier (Plenum, New York, 1976), p. 61.

[8]A. Zangwill and Paul Soven, Phys. Rev. Lett. 45, 204 (1980).

[9]V. V. Afrosimov, Yu S. Gordeev, V. M. Lavrov, and S. G. Shchemelinin, Zh. Eksp. Teor. Fiz. 55, 1569 (1968) [Sov. Phys.—JETP 28, 821 (1969)].

[10]S. E. Schnatterly, in *Solid State Physics,* Vol. 34, edited by H. Ehrenreich, R. Seitz, and D. Turnbull (Academic, New York, 1979).

[11]P. C. Gibbons, J. J. Ritsko, and S. E. Schnatterly, Rev. Sci. Instrum. 46, 1546 (1975).

[12]For some of the fits discussed in this work, we used CURFIT in P. R. Bevington, *Data Reduction and Error Analysis for the Physical Sciences* (McGraw-Hill, New York, 1969), p. 237; and a program due to E. Groth, Princeton University (unpublished).

[13]J. A. Bearden and J. S. Thomsen, in *American Institute of Physics Handbook,* edited by D. E. Gray, 3rd

ed. (McGraw-Hill, New York, 1972), pp. 7–158.
[14]C. P. Franck, Ph.D. thesis, Physics Department, Princeton University, University Microfilms, Ann Arbor, Michigan, 1978 (unpublished) and J. R. Fields, Ph.D. thesis, Physics Department, Princeton University, University Microfilms, Ann Arbor, Michigan, 1975 (unpublished).
[15]T. S. Moss, Proc. Phys. Soc., London, Sect. B. 65, 62 (1952); P. A. Hartig and J. L. Loferski, J. Opt. Soc. Am. 44, 17 (1954).
[16]B. Sonntag, T. Tuomi, and G. Zimmerer, Phys. Status Solidi B 58, 101 (1973).
[17]S. Engelsberg, Phys. Rev. 126, 1262 (1962).
[18]F. Wooten, *Optical Properties of Solids* (Academic, New York, 1972).
[19]*CRC Handbook of Chemistry and Physics,* 60th ed., edited by Robert C. Weast (Chemical Rubber, Boca Raton, Florida, 1980).
[20]We use principles given by J. Orear, Report No. UCRL-8417 (Radiation Laboratory, University of California, Berkeley, 1958).
[21]M. Ya Amusia and N. A. Cherepkov, Case Stud. At. Phys. 5, 47 (1975).
[22]P. M. Platzman and P. A. Wolff, *Waves and Interactions in Solid State Plasmas,* supplement 13 in *Solid State Physics,* edited by H. Ehrenreich, F. Seitz, and D. Turnbull (Academic, New York, 1973), p. 1.
[23]D. Park, *Introduction to the Quantum Theory* (McGraw-Hill, New York, 1964), p. 68.
[24]F. Herman and S. Skillman, *Atomic Structure Calculations* (Prentice-Hall, Englewood Cliffs, New Jersey, 1963).
[25]A. Sen and E. G. Harris, Phys. Rev. A 3, 1815 (1971); B. Kh. Ishmukhametov, Phys. Status Solidi B 45, 669 (1971); G. Wendin, J. Phys. B 4, 1080 (1971); 5, 110 (1971); S. Lundqvist, in *Elementary Excitations in Solids, Molecules and Atoms,* edited by J. T. Devreese, A. B. Kunz, and T. C. Collins (Plenum, New York, 1974), Part A, p. 281.
[26]P. V. Giaquinta, E. Tosatti, and M. P. Tosi, Solid State Commun. 19, 123 (1976); P. V. Giaquinta, M. Parrinello, E. Tossati, and M. P. Tosi, J. Phys. C 9, 2031 (1976).
[27]A. Lucas, in *Elementary Excitations in Solids, Molecules and Atoms,* edited by J. T. Devreese, A. B. Kunz, and T. C. Collins (Plenum, New York, 1974), Part A, p. 65.
[28]D. Pines, *Elementary Excitations in Solids* (Benjamin, New York, 1964), p. 144.
[29]C. Kittel, *Introduction to Solid State Physics,* 4th ed. (Wiley, New York, 1971).
[30]J. C. Ashley and T. L. Ferrell, Phys. Rev. B 14, 3277 (1976).
[31]J. C. Ashley, T. L. Ferrell, and R. H. Ritchie, Phys. Rev. B 10, 554 (1974).
[32]P. M. Platzman, in *Elementary Excitations in Solids, Molecules and Atoms,* edited by J. T. Devreese, A. B. Kunz, and T. C. Collins (Plenum, New York, 1974), Part A, p. 31.